JOURNAL OF NANO- AND ELECTRONIC PHYSICS
Vol. **16** No 5, 05033(5pp) (2024)

ЖУРНАЛ НАНО- ТА ЕЛЕКТРОННОЇ ФІЗИКИ
Том **16** № 5, 05033(5cc) (2024)

OPEN ACCESS

REGULAR ARTICLE

Electronic and Magnetic Properties of the Wurtzite Solid Solution Mn:ZnSeS

S.V. Syrotyuk*, A.Y. Nakonechnyi, Yu.V. Klysko, M.V. Stepanyak, V.M. Myshchyshyn

Lviv Polytechnic National University, 79013 Lviv, Ukraine

(Received 23 June 2024; revised manuscript received 15 October 2024; published online 30 October 2024)

The the structural, electronic, and magnetic characteristics of the ZnSeS solid solution with manganese impurity have been evaluated within the DFT using the hybrid exchange-correlation functional PBE0. The structure of this solid solution was determined in two stages. At the first step the internal coordinates of atoms are optimized, and at the second one the lattice parameter relaxation, including re-optimization of internal coordinates, were done. Further, after the introduction of Mn substitution impurity, electronic energy spectra and the electronic DOS were obtained. Significant changes in parameters of the electronic structure and magnetic properties caused by the manganese impurity were found. It was established that the doped solid solution Mn:ZnSeS is a semiconductor for both electron spin polarizations.

Keywords: ZnSeS solid solution, Mn impurity, Electronic energy bands, DOS, Magnetic moment.

DOI: 10.21272/jnep.16(5).05033 PACS numbers: 71.15.Mb, 71.20.Nr, 71.27. + a

1. INTRODUCTION

The mixed crystals A2B6 have found many applications, namely in development of detecting devices for introscopic systems and in multi-energy X-ray radiography [1].

The limited solubility of components is an obstacle to the production of ZnS_xTe_{1-x} solid solutions. Among various A2B6 materials, $ZnSe_{1-x}S_x$ solid solutions are very interesting, because their components show an unlimited solubility.

Changing the ZnS/ZnSe ratio for $ZnSe_{1-x}S_x$ single crystals gives a possibility for tuning their properties, namely a band gap region, $2.87 \le \varepsilon_g \le 3.93$ eV [2], including their structural, electronic and optical characteristics [3].

A_2B_6 crystals doped with transition 3d elements acquire properties that are important in view of their practical application. The materials, radiating at different wavelengths in visible region (different color from blue to red), have been prepared by doping ZnS, ZnO wit h Cu, Mn and Co transition elements [4].

The yellow-orange band at around 582 nm and 603 nm corresponding to bulk sample ZnS:Mn and nanocrystalline sample ZnS:Mn are characterized by the radiation transition of electrons in 3*d* shell of Mn^{2+} ions.

The 693 nm band of bulk sample ZnO:Co is characterized by the radiation transition of electrons in 3d shell of Co^{2+}.

ZnS:Cu, ZnS:Mn samples reveal the extend luminescence. The lifetime of electrons at excited states 4T1 is about 1.90 ms, 0.79 ms corresponding to bulk, nanocrystalline samples ZnS:Mn. For bulk sample ZnS:Cu, the lifetime of electrons in conduction band is about 8.60 μs [4].

Copper-alloyed ZnS as a *p*-type transparent conducting material (TCM) has been reported in a work [5]. The formation of Cu-alloyed ZnS is thermodynamically unfavorable but non-equilibrium phases have been well known to be synthesizable by a host of techniques such as sputtering, molecular beam epitaxy, and pulsed laser deposition.

A *p*-type wurtzite TCM was synthesized from earth abundant elements. The potential application of this TCM was demonstrated through its use in a rectifying transparent diode. By utilizing a wurtzite transparent *p*-type conductor, photovoltaic cells could potentially be manufactured using new types of materials. In addition, the development and optimization of such a *p*-type TCM could open new frontiers in the development of transparent transistors, light emitting diodes, electrochromic windows, and a wide range of additional optoelectronic devices.

Divalent transition metal ions (TM^{2+}) doped II-VI semiconductors are considered as promising laser gain media and optoelectronic materials in mid-infrared (MIR) region owing to their desirable qualities such as large absorption and emission bandwidth, large emission cross sections and low energy optical phonon cut-off [6]. Cr doped ZnSe is one of the most important member of these materials and has been demonstrated covering a broad range of regimes of operation and output parameters. Recently, nanocrystalline Cr doped ZnSe semiconductor nanowires have been successfully fabricated for the first time, and showed strong emission at around 2000-2500 nm under excitation of 1300-2250 nm wavelength at room temperature.

Peculiarities of the impact of transition 3*d* elements impurities on the electronic structure of wide-gap cubic crystals were studied in theoretical works [7-9].

ZnS and ZnSe crystals, doped with transition 3*d* el-

* Correspondence e-mail: stepan.v.syrotiuk@lpnu.ua

Cite this article as: S.V. Syrotyuk et al., *J. Nano- Electron. Phys.* 16 No 5, 05033 (2024) https://doi.org/10.21272/jnep.16(5).05033

ements, are well-studied materials [10]. Recently the structural and electronic properties of the random alloy ZnSeS have been investigated via density functional theory (DFT) based on the GGA-PBE calculation *s* [11].

However, there is very little information in scientific periodicals about the solid solutions ZnSeS with 3*d* transition impurities. The experimental work is devoted to the excitation wavelength tuning of luminescent Mn^{2+}-doped ZnS_xSe_{1-x} obtained by mechanically induced self-sustaining reaction [12].

However, there are very few publications dedicated to the electronic structure of solid solutions ZnSeS with impurities of transitional elements. This work aims to get new results for mentioned materials, which are currently absent in periodicals.

2. CALCULATION

2.1 The Structure Optimization

The electronic structure of ZnSeS solid solutions doped with Mn atoms was calculated using the ABINIT complex of programs [13] in two stages.

At the first stage, structural optimization was done, which also consisted of two steps. The first step was to optimize the lattice parameter, and the second was to find the precise coordinates of the atoms in the supercell. In order to save space, we present the optimization results for the $Zn_4Se_2S_2$ supercell, which contains eight atoms. The corresponding results are shown in Table 1.

Table 1 – An example of optimizing the structure of a smaller supercell of a $Zn_4Se_2S_2$ solid solution

Coords	*x*/*a*	*y*/*b*	*z*/*c*
S initial	0	0	0.18737
S optimized	0	0	0.19284
S initial	0.33333	0.66667	0.43753
S optimized	0.33333	0.66667	0.43303
Se initial	0	0	0.68737
Se optimized	0	0	0.68130
Se initial	0.66667	0.33333	0.93753
Se optimized	0.66667	0.33333	0.94183
Zn initial	0	0	0
Zn optimized	0	0	0.010976
Zn initial	0.33333	0.66667	0.25000
Zn optimized	0.33333	0.66667	0.25015
Zn initial	0	0	0.5
Zn optimized	0	0	0.48944
Zn initial	0.66667	0.33333	0.75
Zn optimized	0.66667	0.33333	0.75036

As can be seen from Table 1, the Zn atoms have reduced *z*-coordinates (*z*/*c*) different from the starting ideal values 0.0, 0.25, 0.5, 0.75, respectively. The optimized values of the lattice lenghts have acquired the following values: $a = b = 7.46510$, $c = 24.49224$ a.u., respectively. The starting lattice lenghts had the values $a = b = 7.43513$, $c = 24.42189$ a.u., respectively. For none of the atoms, the condition of fixing the reduced coordinates was not applied. And the lattice angles remained the same as in the ideal starting supercell, i.e. $\alpha = \beta = 90$, $\gamma = 120$ degrees, respectively. The Cartesian forces (– 0.00373, 0.000912, 0.00156, 0.00564, 0.00354, – 0.00150, 0.00937, – 0.00451) eV/Å, acting on the two S, two Se and four Zn atoms, respectively, have been reached at the end of a final iteration loop. The corresponding pressure is characterized by a value of 0.0025 GPa. The starting values of the Cartesian forces were equal to (0.0434, – 0.0915, – 0.142, 0.0900, 0.670, 0.0238, – 0.609, 0.0152) eV/Å, respectively. The corresponding starting pressure is characterized by the value of 0.96 GPa.

In this work, we performed all calculations for the $Zn_{31}Mn_1Se_{16}S_{16}$ supercell, which consists of 64 atoms.

2.2 Details of the Calculation Scheme

Electronic structure calculation methods, such as APW, LAPW, and LMTO, are based on the use of MT (spherical-cell, muffin-tin) potentials, i.e., they also involve augmentation of the wave function on the boundary of the augmentation sphere in order to ensure its continuity. The augmentation procedure results in quite complex mathematical calculations, which require significant additional computational costs. The methods mentioned here operate only with numerical arrays of wave functions, electron densities, and crystal potential. These approaches to calculating the electronic structure of crystals are purely numerical.

Difficulties inherent in numerical methods of electronic structure are overcome in basic methods. Calculations of the electronic structure were performed here in the PAW basis (projector augmented waves) [14]. The PAW approach has common features with numerical methods and pseudopotentials. However, pseudopotentials make it possible to obtain a pseudowave function, which is not suitable for the calculation of dipole matrix elements, which are necessary for application in programs for studying optical coefficients and kinetic properties of materials.

At the first stage of the PAW calculation scheme, a smooth pseudo-wave function $|\tilde{\psi}_{\alpha\mathbf{k}}>$ is evaluated. The purpose of the second stage of the calculation in the PAW basis is to obtain the true all-electronic wave function $|\psi_{\alpha\mathbf{k}}>$ of the crystal. Here α is a band index, and $\mathbf{k}$ is a vector from the first Brillouin zone. The true all-electronic wave function is derived by acting of the operator τ on the smooth pseudo-wave function [14],

$$|\psi_{\alpha\mathbf{k}}>=\tau|\tilde{\psi}_{\alpha\mathbf{k}}>. \qquad (2)$$

This operator is built of functions obtained for the free atom. In particular, these functions are partial atomic waves φ, pseudowaves $\tilde{\varphi}_i$ and projectors $\tilde{p}_i$. So, the operator τ looks like this [14],

$$\tau = 1 + \sum_i (|\varphi_i> - |\tilde{\varphi}_i>) < \tilde{p}_i|. \qquad (3)$$

The Schrödinger equation on the plane wave basis is represented by the Hamiltonian matrix *H*. After using the definitions (2), (3) the eigenvalues task for Hamiltonian H turns into the problem of the eigenfunctions and eigenvalues for the matrix of the effective Hamiltonian H_{eff}, whose electronic energy spectrum $\varepsilon_{\alpha\mathbf{k}}$ coin-

cides with that of the H matrix, namely

$$H_{eff} \mid \tilde{\psi}_{\alpha\mathbf{k}} >= \tau^{+}\tau \mid \tilde{\psi}_{\alpha\mathbf{k}} > \varepsilon_{\alpha\mathbf{k}} . \quad (4)$$

Here the effective Hamiltonian $H_{eff} = \tau^{+} H \tau$ is derived from the all-electronic Hamiltonian H. The true all-electronic function $\psi_{\alpha\mathbf{k}}$ is suitable for calculation the dipole matrix elements necessary to obtain the optical constants of crystals [15, 16] and the kinetic coefficients of semiconductors [17].

The strongly correlated 3d electrons of the Mn atom move in narrow energy bands and are characterized by large effective mass values. This means that the usual exchange-correlation functional PBE [18], which takes into account the gradient corrections of the electron density, is not suitable for an adequate description of 3d electrons. That is why we use the hybrid exchange-correlation functional PBE0 here. The latter is employed in the following form [19], namely

$$E_{xc}^{PBE0}[\rho] = E_{xc}^{PBE}[\rho] + \beta(E_{x}^{HF}[\Psi_{3d}] - E_{x}^{PBE}[\rho_{3d}]) . (5)$$

In this functional, the exchange-correlation energy of the 3d electrons of the Mn atom E_{x}^{PBE}, found in the GGA approximation, is partially removed, and the exchange energy of the same electrons, found in the Hartree-Fock theory E_{x}^{HF}, is substituted in its place.

Namely, the PBE0 functional is a mixture of two exchange-correlation functionals. The first of them is the usual GGA functional. It is suitable for smoothly varying electron densities in space. The second term in Eq. (5) contains the Hartree-Fock energy, in which there is no self-interaction error, which is very large for electrons that move in narrow energy bands, namely 3d electrons. The mixing factor β is recommended to be 0.25 [19]. The importance of using the hybrid exchange-correlation functional PBE0 was confirmed in a recent study of a solid solution of ZnSeTe with an admixture of a chromium 3d element [20], including a cationic vacancy.

3. RESULTS AND DISCUSSION

The calculated electronic properties of the Mn:ZnSeS solid solution in which the Mn atom replaces the Zn atom, are shown in Figures 1-8.

Fig. 1 shows the majority-spin electronic energy bands. As can be seen from this Figure the Fermi level is situated within the forbidden band gap. So, the material Mn:ZnSeS represented by asupercell $Zn_{31}Mn_{1}Se_{16}S_{16}$ reveals the semiconductor properties for the spin-up charge carriers. This is the direct-gap semiconductor with a bandgap of 1.36 eV.

Fig. 2 shows the minority-spin electronic energy bands. As can be seen from this Figure the Fermi level is also situated within the forbidden band gap. So, the material Mn:ZnSeS represented by asupercell $Zn_{31}Mn_{1}Se_{16}S_{16}$ reveals the semiconductor properties for the spin-down charge cariers. This is the direct-gap semiconductor with a bandgap of 1.73 eV.

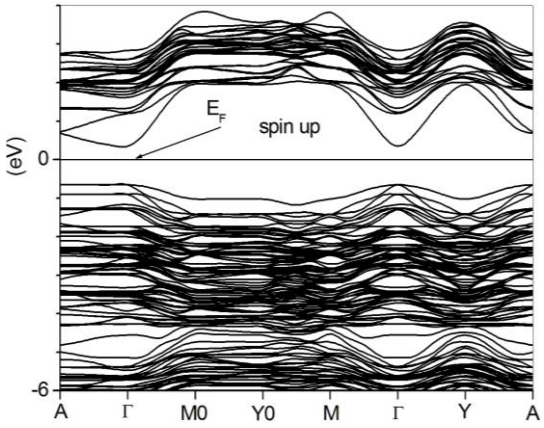

Fig. 1 – The majority-spin electronic energy bands, evaluated for supercell $Zn_{31}Mn_{1}Se_{16}S_{16}$

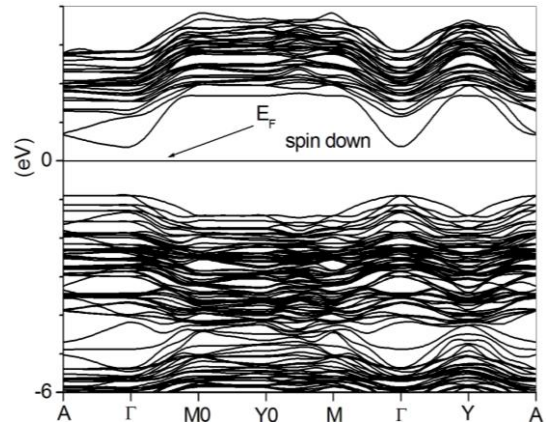

Fig. 2 – The minority-spin electronic energy bands, evaluated for supercell $Zn_{31}Mn_{1}Se_{16}S_{16}$

The partial densities of states on Zn atom, presented in Fig. 3, show that the valence band is formed mainly by d and p atomic states. However, Zn atoms mainly delegate s states to the conduction zone.

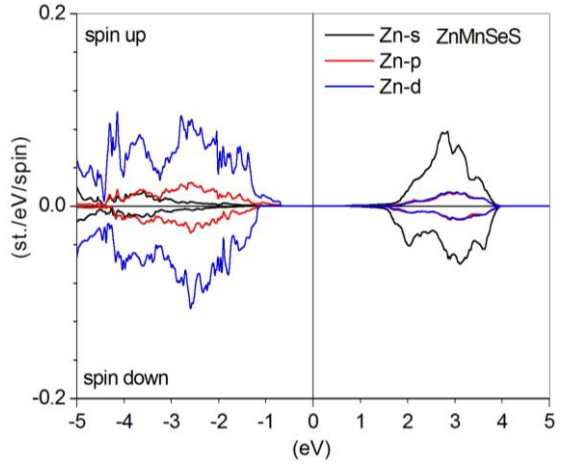

Fig. 3 – The spin-resolved partial DOS, evaluated for supercell $Zn_{31}Mn_{1}Se_{16}S_{16}$

Curves in Fig. 4 reveal a significant asymmetry of the Mn d states, which indicates the presence of a non-zero magnetic moment of the supercell. The latter equals to 5.0μ_B and the Mn atom contribution is 3.8μ_B. We also note in Fig. 4 narrow energy bands of d sym-

metry in the valence band, which are characterized by large values of the density of electronic states. For an adequate description of such states, we employ the PBE0 hybrid exchange-correlation functional. The usual GGA functional is unsuitable for describing electrons that move in narrow energy bands of *d*(*f*) symmetry. It is these charge carriers that are characterized by a large amount of self-interaction energy, which is partially excluded in the PBE0 functional.

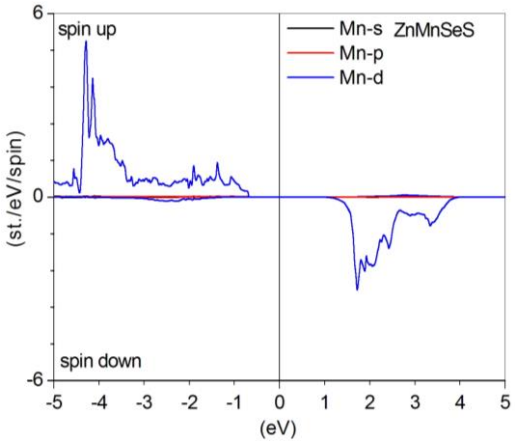

Fig. 4 – The spin-resolved partial DOS, evaluated for supercell $Zn_{31}Mn_1Se_{16}S_{16}$

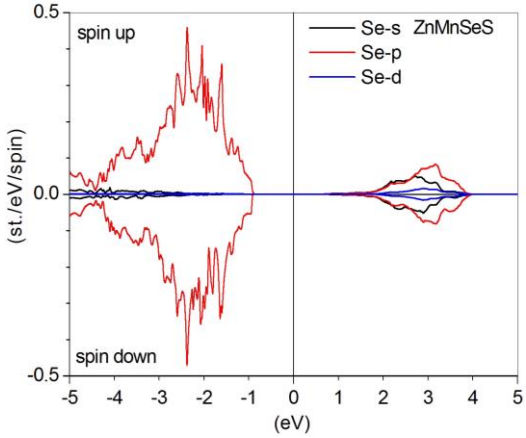

Fig. 5 – The spin-resolved partial DOS, evaluated for supercell $Zn_{31}Mn_1Se_{16}S_{16}$

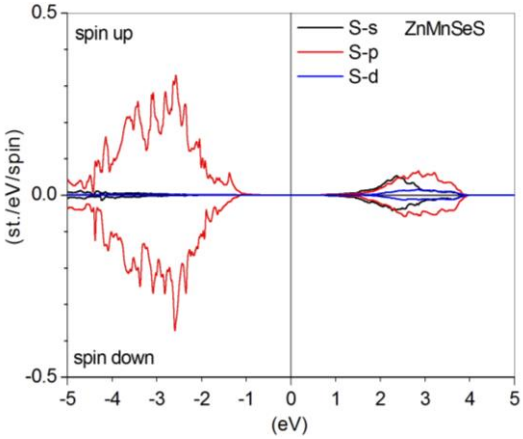

Fig. 6 – The spin-resolved partial DOS, evaluated for supercell $Zn_{31}Mn_1Se_{16}S_{16}$

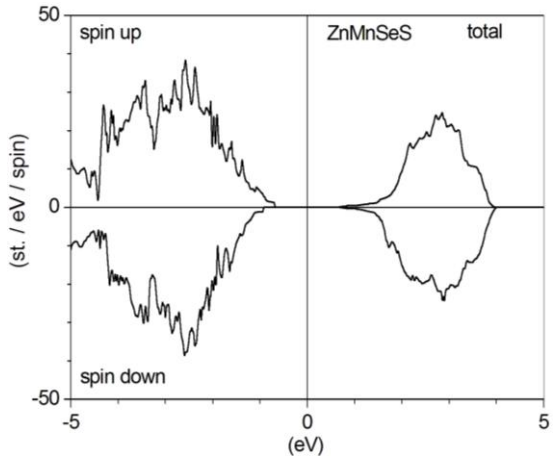

Fig. 7 – The spin-resolved total DOS, evaluated for supercell $Zn_{31}Mn_1Se_{16}S_{16}$

The results shown in Figures 5 and 6 represent the partial DOS on Se and S atoms. As can be seen from these figures, qualitatively the densities of partial electronic states are close. The predominance of p states in the valence band is also a common feature of these graphs.

The asymmetry of the partial DOS curves is the result of the effect of the transition element Mn on the polarization of the electron density even on such nonmagnetic elements as Se and S. The asymmetry of the partial DOS mentioned here is also characteristic for the Zn atom (see Fig. 3).

4. CONCLUSIONS

At the first one, the spin-polarized electronic structure of the Mn:ZnSeS solid solution is investigated.

Electronic energy bands were evaluated for $Zn_{31}Mn_1Se_{16}S_{16}$ supercell in which the Zn atom is replaced by the Mn atom. The calculation results revealed significant changes in the electronic structure due to the presence of manganese impurity. Thus, the electronic energy spectrum of charge carriers with spin up is characterized by an interband optical gap of 1.36 eV. And for carriers with an opposite spin states, this parameter is equal to 1.73 eV.

ACKNOWLEDGEMENTS

This contribution was created under the support of the High Performance Computing Laboratory at the Lviv Polytechnic National University.

REFERENCES

1. O.G. Trubaieva, M.A. Chaika, A.I. Lalayants, *Lith. J. Phys.* **58**, 254 (2018).
2. I. Hernández-Calderón, *II-VI Semiconductor Materials and their Applications* (Ed. by M.C. Tamargo) (Taylor and Francis New York: 2002).
3. M. Rabah, B. Abbar, Y. Al-Douri, B. Bouhafs, B. Sahraoui, *Mater. Sci. Eng. B* **100**, 163 (2003).
4. Pham Van Ben, Phan Trong Tue, *VNU Journal of Science, Mathematics – Physics* **24**, 181 (2008).
5. A.M. Diamond, L. Corbellini, K. R. Balasubramaniam, S. Chen, S. Wang, T.S. Matthews, L.-W. Wang, R. Ramesh, J.W. Ager, *phys. status solidi* a **209**, 2101 (2012).
6. S. Dai, G. Feng, Y. Zhang, L. Deng, H. Zhang, S. Zhou, *Res. Phys.* **8**, 628 (2018).
7. S.V. Syrotyuk, V. M. Shved, *Condens. Matter Phys.* **16**, 13701 (2013).
8. M. Labair, H. Rached, D. Rached, S. Benalia, B. Abidri, R. Khenata, R. Ahmed, S. Bin Omran, A. Bouhemadou, S.V. Syrotyuk, *Int. J. Modern Phys. C* **27**, 1650107 (2016).
9. S.V. Syrotyuk, I.V. Semkiv, H.A. Ilchuk, V.M. Shved, *Condens. Matter Phys.* **19**, 43703 (2016).
10. S.B. Mirov, I.S. Moskalev, S. Vasilyev, V. Smolski, V.V. Fedorov, D. Martyshkin, J. Peppers, M. Mirov, A. Dergachev, V. Gapontsev, *IEEE J. Selected Topics Quantum Electron.* **24**, 1601829 (2018).
11. S. Sarkar, O. Eriksson, D.D. Sarma, I. Di Marco, *Phys. Rev. B* **105**, 184201 (2022).
12. M.A. Avilés, F.J. Gotor, *Opt. Mater.* **117**, 111121 (2021).
13. X. Gonze, F. Jollet, F. Abreu Araujo, D. Adams, B. Amadon, T. Applencourt, C. Audouze, J.-M. Beuken, J. Bieder, A. Bokhanchuk, E. Bousquet, F. Bruneval, D. Caliste, M. Cote, F. Dahm, F. Da Pieve, M. Delaveau, M. Di Gennaro, B. Dorado, C. Espejo, G. Geneste, L. Genovese,A. Gerossier, M. Giantomassi, Y. Gillet, D.R. Hamann, L. He, G. Jomard, J. Laflamme Janssen, S. Le Roux, A. Levitt, A. Lherbier, F. Liu, I. Lukacevic, A. Martin, C. Martins, M.J.T. Oliveira, S. Ponce, Y. Pouillon, T. Rangel, G.-M. Rignanese, A.H. Romero, B. Rousseau, O. Rubel, A.A. Shukri, M. Stankovski, M. Torrent, M.J. Van Setten, B. Van Troeye, M.J. Verstraete, D. Waroquier, J. Wiktor, B. Xu, A. Zhou, J.W. Zwanziger, *Comput. Phys. Commun.* **205**, 106 (2016).
14. P.E. Blöchl, *Phys. Rev.* **B 50**, 17953 (1994).
15. S.V. Syrotyuk, Yu.V. Klysko, *J. Nano Electron. Phys.* **12**, No 5, 05018 (2020).
16. M. Boukhtouta, Y. Megdoud, S. Benlamari, H. Meradji, Z. Chouahda, R. Ahmed, S. Ghemid, Mohammed Abu-Jafar, S. Syrotyuk, D.P. Rai, S. Bin Omran, R. Khenata, *Philosoph. Mag.* **100** No 9, 1150 (2020).
17. O.P. Malyk, S.V. Syrotyuk, *J. Nano- Electron. Phys.* **14** No 1, 01014 (2022).
18. J.P. Perdew, K. Burke, M. Ernzerhof, *Phys. Rev. Lett.* **77** 3865 (1996).
19. F. Tran, P. Blaha, K. Schwarz, P. Novák, *Phys. Rev.* B **74**, 155108 (2006).
20. S.V. Syrotyuk, A.Y. Nakonechnyi, Yu.V. Klysko, Z.E. Veres, I.I. Lahun, *J. Nano- Electron. Phys.* **16** No 1, 01016 (2024).

Електронні та магнітні властивості вюрцитового твердого розчину Mn:ZnSeS

С.В. Сиротюк, А.Й. Наконечний, Ю.В. Клиско, М.В. Степаняк, В.М. Мищишин

Національний університет «Львівська політехніка», 79013 Львів, Україна

Оцінено структурні, електронні та магнітні характеристики твердого розчину ZnSeS з домішкою марганцю в рамках DFT з використанням гібридного обмінно-кореляційного функціоналу PBE0. Структуру цього твердого розчину визначали в два етапи. На першому кроці оптимізуються внутрішні координати атомів, а на другому – релаксація параметрів решітки, включаючи повторну оптимізацію внутрішніх координат. Далі, після введення домішки заміщення Mn, були отримані електронні енергетичні спектри та густини електронних станів ГЕС, DOS. Виявлено суттєві зміни параметрів електронної структури та магнітних властивостей, зумовлені домішкою марганцю. Було встановлено, що легований твердий розчин Mn:ZnSeS є напівпровідником для обидвох спінових поляризацій електронів.

Ключові слова: Твердий розчин ZnSeS, Домішка Mn, Електронні енергетичні зони, ГЕС (DOS), Магнітний момент.